Biosensors and Bioelectronics 74 (2015) 612–627

Contents lists available at ScienceDirect

Biosensors and Bioelectronics

journal homepage: www.elsevier.com/locate/bios

Recent advances in nanoparticle based aptasensors for food contaminants

Richa Sharma [a,b], K.V. Ragavan [a,b], M.S. Thakur [c,*], K.S.M.S. Raghavarao [a,b,**]

[a] Department of Food Engineering, CSIR-CFTRI, India
[b] Academy of Scientific and Innovative Research, India
[c] Materials Science Centre, University of Mysore, Mysore 570005, Karnataka, India

ARTICLE INFO

Article history:
Received 1 April 2015
Received in revised form
6 July 2015
Accepted 10 July 2015
Available online 11 July 2015

Keywords:
Aptamers
Nanoparticles
Food contaminants
Biosensors
Food safety

ABSTRACT

Food safety and hazard analysis is a prime concern of human life, thus quality assessment of food and water is the need of the day. Recent advances in nano-biotechnology play a significant role in providing possible solutions for developing highly sensitive and affordable detection tools for food analysis. Nanomaterials based aptasensors hold great potential to overcome the drawbacks of conventional analytical techniques. Aptamers comprise a novel class of highly specific bio-recognition elements which are produced by SELEX (systematic evolution of ligands by exponential enrichment) process. They bind to target molecules by folding into 3D structures that can discriminate different chiral compounds. The flexibility in making modifications in aptamers contribute to the design of biosensors, enabling the generation of bio-recognition elements for a wide variety of target molecules. Nanomaterials such as metal nanoparticles, metal nanoclusters, metal oxide nanoparticles, metal and carbon quantum dots, graphene, carbon nanotubes and nanocomposites enable higher sensitivity by signal amplification and introduce several novel transduction principles such as enhanced chemiluminescence, fluorescence, Raman signals, electrochemical signals, enhanced catalytic activity, and super-paramagnetic properties to the biosensor. Although there are a few reviews published recently which deal with the potential of aptamers in various fields, none are devoted exclusively to the potential of aptasensors based on nanomaterials for the analysis of food contaminants. Hence, the current review discusses several transduction systems and their principles used in aptamer based nanosensors which have been developed in the past five years, the challenges faced in their designing, along with their strengths and limitations.

Contents

Abbreviations: ABEI, N-(4-aminobutyl)-N-ethyl-isoluminol; AgNC, Silver nanoclusters; AgNPs, Silver nanoparticles; ATP, Adenosine 5′-triphosphate; AuNPs, Gold nanoparticles; AuRu, Gold–ruthenium; BPA, Bisphenol A; cfu, Colony forming units; CL, Chemiluminescence; CNT, Carbon nanotubes; CRET, Chemiluminescence resonance energy transfer; CTAB, Cetyltrimethylammonium bromide; DTNB, 5,5′-dithiobis-(2-nitrobenzoic acid); ECL, Electrochemiluminescence; EDTA, Ethylenediaminetetraacetic acid; FAM, Carboxyfluorescein; FO-SPR, Fibre optic-surface plasmon resonance; FRET, Fluorescence resonance energy transfer; GO, Graphene oxide; HRP, Horseradish peroxidase; IR, Infrared; LOD, Limit of detection; MNP, Magnetic nanoparticles; NC, Nanoclusters; NP, Nanoparticles; ODI-CL, 1, 1′-oxalyldiimidazole chemiluminescence; OTA, Ochratoxin A; OTC, Oxytetracycline; PCR, Polymerase chain reaction; PDDA, Poly(diallyldimethylammonium); PDMS, Poly(dimethylsiloxane); ppb, Parts per billion; ppm, Parts per million; ppt, Parts per trillion; PVP, poly(vinyl pyrrolidone); QD, Quantum dots; qPCR, Quantitative polymerase chain reaction; RRS, Resonance Rayleigh Scattering; RS, Rayleigh scattering; SEB, Staphylococcal enterotoxin B; SELEX, Systematic evolution of ligands by exponential enrichment; SERRS, Surface enhanced Resonance Raman scattering; SERS, Surface enhanced Raman scattering; SPR, Surface plasmon resonance; ssDNA, Single strand deoxyribonucleic acid; SWCNT, Single walled carbon nanotubes; TET, Tetracycline; T–Hg^{2+}–T, Thymine–mercury ions–thymine bond; UCNP, Up-conversion nanoparticle; UV, Ultraviolet

* Corresponding author.
** Corresponding author at: Department of Food Engineering, CSIR-Central Food Technological Research Institute, Mysore 570020, Karnataka, India. Fax: +91 821 2517233.
E-mail addresses: msthakur@yahoo.com (M.S. Thakur), raghavarao@cftri.res.in (K.S.M.S. Raghavarao).

http://dx.doi.org/10.1016/j.bios.2015.07.017
0956-5663/

1. Introduction

1.1. Purpose of the review

With increased globalization of food supply, the need for stringent food regulations and safety measures have taken prime position amongst health concerns. Unsafe food can be linked to an estimated 2 million deaths annually, including children. Food contaminated with harmful pathogens, microbes or chemical substances leads to more than 200 diseases. Food safety is threatened by new challenges, for example, changes in procedures for production and distribution, altered food habits, emerging pathogens and increased contamination due to rise in travel and trade, among others. Quite evidently, the World Health Organization (WHO), has decided food safety as their agenda on the World Health Day, 7 April 2015. According to WHO experts, food safety measures require implementation of necessary actions in all stages of food production – harvest, transport, processing, storage and preparation (World Health Organization, 2015).

Ensuring food safety to the global public is a prime challenge for regulatory bodies and the scientific community. The inadequacy of conventional methods calls for novel and reliable techniques to enable convenient, high-speed and sensitive analysis of food contaminants and nutrients. Modern biotechnology presents new opportunities for accurate and affordable food diagnostics, employing specific target-binders coupled with efficient transducing systems. Aptamers are such bio-recognition elements that can be attached to reporters and linkers to enable direct signal transduction, such as optical, electrochemical or piezoelectric sensing modalities. They possess additional properties such as conformational change on analyte-binding, high specificity for single target analyte and sequence modification which open up a plethora of possible detection methodologies. Nanotechnology adds on to the applicability and convenience of these analytical strategies. Basic and application aspects of nanotechnology were studied extensively in the last decade which led to rise of nanomaterials as powerful tools not only for the development of novel biosensing techniques but also for the improvement of existing detection platforms. Nanomaterials, due to their high surface area, increase the functional surface of the device and thus lead to higher sensitivity, the most vital aspect of a biosensor. The present review focuses on the recent analytical techniques that employ the unique physicochemical advantages of nanomaterials as efficient signal transducers and amplifiers, in conjunction with the selectivity and flexibility of aptamers (Scheme 1). These potent nanomaterial based aptasensors have revolutionized the technology of detection and will continue to do so for coming years. The review summarizes the significant developments in this direction over the last five years and aims to provide an insight into the science and technology of aptamer aided nanosensors.

2. Components of aptasensor

Nanoparticle based aptasensors mainly comprise of aptamers (the target-recognition elements) and nanomaterials (the signal transducers and/or signal enhancers). The roles of these components are explained below.

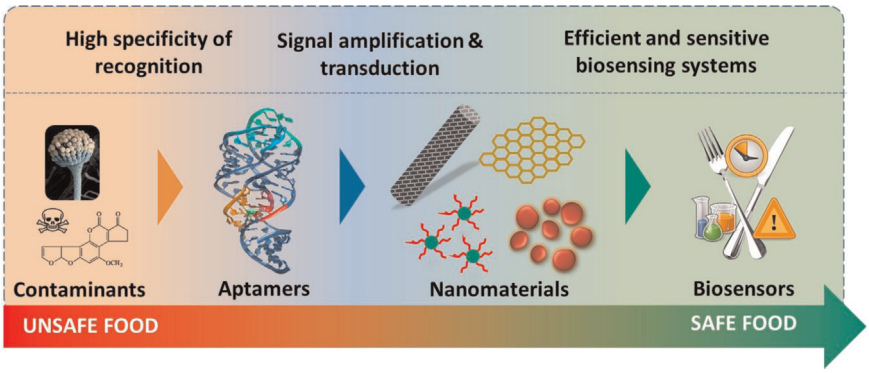

Scheme 1. Schematic representation of contribution of aptamers and nanomaterials in development of sensitive and efficient biosensors for food safety analysis.

2.1. Aptamers

Aptamers are single stranded nucleic acid or peptide molecules of size less than 25 kDa which can be natural or synthetic by origin. Aptamers are highly specific and selective towards their target compounds, namely, ions, proteins, toxins, microbes and viruses, due to their precise and defined three-dimensional structures (Mayer, 2009; Radom et al., 2013), with superior physical and chemical attributes than antibodies (Smuc et al., 2013). Aptamers are termed as synthetic antibodies because of their selection and generation through an in vitro combinatorial molecular technique called SELEX. In brief, a nucleotide sequence with high specificity towards a target is selected from a large pool of sequences (usually $\sim 10^{15}$) based on affinity between the aptamer and the target (Tuerk and Gold, 1990; Klug and Famulok, 1994). Dissociation constants of aptamers are reported in the nanomolar to picomolar range, superior to monoclonal antibodies in some cases (Song et al., 2008; Iliuk et al., 2011). Hence, they are extensively used as recognition elements in the fabrication of aptasensors and diagnostic kits based on electrochemical, chemiluminescence, fluorescence and piezoelectric principles (Cho et al., 2009; Iliuk et al., 2011; Hong et al., 2012). Recently published literature highlights the potential of aptamers in food safety and quality analysis (Yadav et al., 2010; Karkkainen et al., 2011; Mehta et al., 2011; McKeague et al., 2011; Campas et al., 2012; Dong et al., 2013; Rhouati et al., 2013). In this review, reports published in the last five years that deal with application of metal, carbon and other nanomaterials in developing aptamer based sensors for detection and analysis of food and water contaminants, toxins and pathogens have been discussed.

2.2. Nanomaterials

Nanoparticles are used extensively in developing assays for the detection of food contaminants (Valdes et al., 2009). Their size-related properties at nano-scale are quantum confinement in semiconductor nano-crystals and surface plasmon resonance in nanoparticles composed of noble metals and their alloys. High surface area to volume ratio, high electrical conductivity, magnetic property and unique physicochemical properties of nanomaterials promote their use in analysis, molecular diagnostics and imaging. In addition to these nanoparticles, other nanomaterials composed of oxides, inorganic compounds or composites play crucial roles in different biosensing systems. They are discussed in the following sections.

2.2.1. Metal nanoparticles and nanoclusters

Metal nanoparticles (5–100 nm) have fascinating physico-chemical and optoelectronic properties at nano-dimensions (Saha et al., 2012; Burris and Stewart, 2012). They are being increasingly used as transducing materials in the fabrication of sensors for the analysis of food contaminants, toxins and pathogens (Sozer and Kokini, 2009; Viswanathan, 2011; Pérez-López and Merkoçi, 2011; Saha et al., 2012). Noble metal nanoparticles are advantageous over other nanomaterials due to ease of functionalization via simple chemistry, high surface area-to-volume ratio, unique spectral and optical properties, redox properties, conductivity and luminescence besides their ability to respond optically and electrochemically to external stimuli.

Metal nanoclusters are ultra-small nanoparticles (<5 nm) containing less than a few hundred atoms of metals such as gold, silver, platinum and copper. Such nanoclusters have tunable fluorescent emission over the visible and near infra-red region which depends on their capping agent, size and synthesis route. Owing to their small size, high photo-stability, high quantum yield, low toxicity and compatibility for bio-conjugation, they are increasingly finding applications in nano-biosensing and cell line imaging, replacing conventional fluorescent organic dyes and semi-conductor quantum dots (Shang et al., 2011).

2.2.2. Semiconductor nanoparticles

Quantum dots (QDs), nanoscale semiconductor fluorescent crystals (<5 nm) composed of compounds formed by Zn and Cd with Te and Se, are suitable for designing nano-probes due to their properties such as size-controlled fluorescence, higher fluorescence quantum yields than dyes, and stability against photobleaching (Gill et al., 2008). QDs offer the convenience of conjugation to aptamers without affecting either their emission properties or aptamer specificity.

2.2.3. Carbon nanoparticles

Carbon nanomaterials, namely, carbon nanotubes (CNTs), graphene quantum dots, graphene and fullerenes are gaining attention in recent times for their exciting properties (Yang et al., 2010; Jariwala et al., 2013). Among them, CNTs and graphene are extensively incorporated in fabrication of sensors for food application (Kochmann et al., 2012; Wang et al., 2012; Najafi et al., 2014). Graphene is a two dimensional (one atom thick) carbon nanomaterial which has good electron conductivity, large surface area, energy acceptance ability and mechanical strength (Guo and Dong, 2011). They are used as fluorescence quenchers (Guo et al., 2011). CNTs are one-dimensional carbon nanomaterials known for their stable chemical, unique electrical, mechanical, thermal and structural properties (Sánchez-Pomales et al., 2009). They are mainly used in the fabrication of electrochemical biosensors. However, their applications in sensors and other fields are disputed due to their toxicity (Liu, Y., et al., 2013).

2.2.4. Other nanoparticles

Several types of nanoparticles differing from the aforementioned groups have been used in biosensors. Among them, magnetic nanoparticles, usually formed from oxides of iron, and up-conversion nanoparticles, comprising of lanthanide series metals, have been used with aptamers for detection of food contaminants. These are discussed in the following sections.

2.2.4.1. Magnetic nanoparticles. Magnetic nanoparticles display supra-paramagnetic property below 50 nm size. Their ability to separate target molecules from other compounds by the simple use of a permanent magnetic field makes them attractive materials for the fabrication of sensors. Recently, it was also demonstrated that they can be used as an electrode modifier to improve the electron conductivity (inherent property of metal oxide nanoparticles). Currently, they are being used with aptamers in food analysis due to this combined advantage of separation of biomolecules and signal enhancement (Cao et al., 2012).

2.2.4.2. Up-conversion nanoparticles (UCNPs). UCNPs belong to a new class of luminescent materials which transform the near infrared radiations (lower energy) into visible radiation (higher energy). UCNPs offer a promising alternative to fluorescent dyes and quantum dots due to low background noise, highly stable emission (resistance to photo-bleaching), sharp emission bands and good penetration of signals in tissues with low absorption (helpful in real time detection and imaging in tissues). They are used as fluorescent labels to tag with aptamers for biosensing of various target compounds. The mechanism and design are discussed later in the review (Wang, M., et al., 2011).

3. Nanomaterial-based aptasensing platforms

A wide variety of transducing systems have been employed in

Table 1
Various aptasensors for food and allied applications.

Target compound	Biosensing principle	Nanoparticles	Detection limit (LOD)	Reference
Pesticides and insecticides				
Isocarbophos	Nanoparticles as Raman labels in SERS	Ag dendrites	3.4 μM	Pang et al. (2014)
Omethoate			24 μM	
Phorate			0.4 μM	
Profenofos			14 μM	
Acetamiprid	Electrochemical aptasensor	AuNPs	1 nM	Fan et al. (2013)
Acetamiprid	Non-crosslinking aggregation	AuNPs	5 nM	Shi et al. (2013)
Antibiotics, drugs and their residues				
Oxytetracycline	Non-crosslinking aggregation	AuNPs	25 nM	Kim et al. (2010)
Kanamycin, kanamycin B, tobramycin		AuNPs	25 nM	Song et al. (2011)
Aminoglycosidic antibiotics		AuNPs	1–100 nM	Derbyshire et al. (2012)
Tetracycline		AuNPs	45.8 nM	He et al. (2013a)
Tetracycline		AuNPs	122 nM	He et al. (2013b)
Lysergamine, Metergoline		AuNPs	–	Rouah-Martin et al. (2012)
Cocaine	FRET	QDs	0.5 μM (signal-off mode)	Zhang and Johnson (2009)
Cocaine	Rolling circle amplification and molecular beacons	AuNPs	0.48 nM	Ma et al. (2011)
Cocaine	Fluorescence and non-crosslinking aggregation	AuNPs	Not specified	Luo et al. (2012)
Kanamycin	Electrochemical aptasensors	Polymer–Au self-assembled nano-composite	9.4 nM	Zhu et al. (2012)
		Chitosan–AuNPs, graphene–AuNPs and multi-walled CNT–cobalt phthalocyanine	5.8 nM	Sun et al. (2014)
Heavy metals				
Mercury (Hg^{2+}) ions	Non-crosslinking aggregation	AuNPs	0.6 nM	Li et al. (2009)
Arsenic (As^{3+}) ions		AuNPs	5.3 ppb	Wu et al. (2012a)
Hg^{2+}	FRET	AuNPs	16 nM	Tan et al. (2013)
Hg^{2+}	CRET	QDs	10 nM	Freeman et al. (2011)
Hg^{2+}	SPR spectroscopy	AuNPs	10 fM	Pelossof et al. (2011)
Hg^{2+}	RRS	AuNPs	0.03 nM	Jiang et al. (2009)
Hg^{2+}		AuNPs	0.1 nM	Wen et al. (2010)
Hg^{2+}		AuNPs	0.034 μg/mL	Jiang et al. (2010)
Hg^{2+}		AuRuNPs	1.5 pmol/L	Liang et al. (2011a)
As^{3+}		AuNPs	0.2 ppb	Wu et al. (2012b)
Hg^{2+}	SERRS	Nanoporous Au films	1 pM	Zhang et al. (2013)
Hg^{2+}	Electrochemical aptasensors	AuNPs	0.5 nM	Zhu et al. (2009)
Cu^{2+}		AuNPs	0.1 pM	Chen et al. (2011)
Microbial cells				
Salmonella typhimurium	Reduction of silver to produce dark colour	AuNPs	7 cfu/mL	Yuan et al. (2014)
Escherichia coli Listeria monocytogenes Salmonella enterica	Chromato-graphic strip based	AuNPs QDs	3000–6000 cells/test (AuNPs) 300–600 cells/test (QDs)	Bruno (2014)
Vibrio parahaemolyticus Salmonella typhimurium	Aptamer based dual colour flow cytometry	QDs	5×10^3 cfu/mL for both	Duan et al. (2013)
C. jejuni	Fluorimetric/luminescence sensors coupled with magnetic separation	QDs MNPs	10–250 cfu	Bruno et al. (2009)
Salmonella typhimurium		UCNPs and Fe_3O_4 MNPs	5 cfu/mL	Duan et al. (2012b)
Staphylococcus aureus			8 cfu/mL	
Vibrio parahaemolyticus	ODI-CL	GO	2230 cells/mL	Kwun et al. (2014)
Staphylococcus aureus	RRS	AuNPs	Single cell	Chang et al. (2013)
Staphylococcus aureus	Luminescence sensors coupled with magnetic separation	UCNPs and Fe_3O_4 MNPs	25 cfu/mL	Wu et al. (2014)
Vibrio parahemolyticus			10 cfu/mL	
Salmonella typhimurium			15 cfu/mL	
Microbial toxins				
OTA	Non-crosslinking aggregation	AuNPs	20 nM	Yang et al. (2011)
OTA	FRET	AuNPs	2×10^{-12} g/mL	Duan et al. (2012a)
OTA		SWCNTs	24.1 nM	Guo et al. (2011)
OTA		Graphene oxide	18.7 nM	Sheng et al. (2011)
OTA		GO and UCNPs	0.02 ng/mL	Wu, S., et al. (2012)
Fumonisin B1			0.1 ng/mL	
OTA	Chromato-graphic strip based	QDs	1.9 ng/mL	Wang et al. (2011a)
OTA		AuNPs	0.18 ng/mL	Wang et al. (2011b)
OTA	Fluorescent reporter binding to analyte	AgNCs	0.5 ng/mL	Chen et al. (2014)
OTA	Fluorimetric sensors coupled with separation by magnetic nanoparticles	QDs γ-Fe_2O_3 MNPs copolymer nanospheres	0.0001 ng/mL	Wu, S., et al. (2011)
OTA	Electrochemiluminescence	AuNPs	0.007 ng/mL	Wang et al. (2010)
OTA	Electrochemical aptasensor	AuNPs	30 pg/mL	Kuang et al. (2010)
OTA	Impedimetric aptasensor	IrO_2 NPs	14 pM	Rivas et al. (2015)
Staphylococcal enterotoxin B	Nanoparticles as Raman labels in SERS	Au nanorods core–shell Fe–	224 aM	Temur et al. (2012)

Table 1 (*continued*)

Target compound	Biosensing principle	Nanoparticles	Detection limit (LOD)	Reference
		AuMNPs		
Other analytes				
BPA	Non-crosslinking aggregation	AuNPs	0.1 ng/mL	Mei et al. (2013)
Theophylline		AuNPs	50 ng/mL	Katiyar et al. (2013)
Melamine		AuNPs	0.5 mg/L	Yun et al. (2014)
Melamine	RRS	AuNPs	0.38 ng/L	Liang et al. (2011c)
		AgNPs	3.1 μg/L	Liang et al. (2011b)
Lysozyme	Fluorescence quenching	GO	Not specified	Lin et al. (2014)
Lysozyme	Reduction of silver to produce dark colour	AuNPs–PDMS nanocomposite film	1×10^{-4} μg/mL	Wang, W., et al. (2011)
ATP			1×10^{-4} μg/mL	
ATP	Fluorescent flow sensor	QDs	5 mM	Bogomolova and Aldissi (2011)
ATP	CRET	QDs	100 nM	Freeman et al. (2011)
Target DNA			1×10^{-8}–1×10^{-9} M	
ATP	CRET	QDs	10 μM	Liu et al. (2011)
Ara h1	Fibre optic SPR	AuNPs	75 nM	Tran et al. (2013)
Ricin	Nanoparticles as Raman labels in SERS	Ag dendrites	10 ng/mL	He et al. (2011)
BPA	Electrochemical aptasensor	AuNP dotted graphene nanocomposite film	5 nM	Zhou et al. (2014)
BPA	SERS	Self-assembled monolayer protected AuNPs	3 nM	Marks et al. (2014)

aptasensors for food quality assessment with their principles being based on the property of the nanoparticles used. The detection formats can be broadly classified into optical and electrochemical systems, while, magnetic particle based separation and detection has also been reported by a few researchers. In this review, various aptasensors have been classified according to the target food analyte as presented in Table 1.

3.1. Optical aptasensors

Optical sensors comprise of transducers that can capture signals in the form of ultraviolet (UV), visible and infrared (IR) radiations from a chemical/biological/physical reaction or event, and can transform them into different data formats. They are further classified as colorimetric, fluorimetric, bioluminescence-based, chemiluminescence-based and surface plasmon resonance-based sensors (McDonagh et al., 2008), based on the light source. A massive proportion of developed biosensors rely on optical transduction owing to the simplicity of operation, rapidity and sensitivity. In this review, these sensing systems and their subdivisions, have been discussed in detail due to their importance in the field of bioanalysis.

3.1.1. Colorimetric nanosensors

Colorimetric nanosensors rely on the size dependent optical properties of nanoparticles, especially gold nanoparticles (AuNPs) that can rapidly change colour in colloid form due to variation in particle size. Electrons near the surface of noble metals oscillate in response to external electromagnetic stimuli. At resonance, the electrons absorb maximum amount of energy – the phenomenon is known as the surface plasmon resonance (SPR). The resonance wavelength is dependent on the size and shape of the particle. In localized SPR, if the size of colloidal NPs is altered due to their aggregation, the absorption wavelength changes. The signal can be observed visually and spectrally, simplifying the procedure and often circumventing the requirement of instruments (discussed below). However, for particles immobilized on surfaces (non-colloidal systems), the attachment of analyte to the surface alters SPR signal (propagating SPR), which can only be measured through a suitable instrument. Further, change in SPR corresponds to change in scattering properties of NPs, which cannot be sensed colorimetrically. Such sensors have been discussed in Section 3.1.4. Colorimetric aptasensors are well-known for qualitative detection of target compounds, and at times they can be semi-quantitative.

Gold nanoparticles and aptamers have been extensively used to design colorimetric sensors for visual detection of food and water contaminants. Most conventional colorimetric sensors rely on the principle of 'non-crosslinking aggregation' mechanism involving change in colloidal state of the AuNPs. Some of the reasons for which this principle has been extensively employed in food analysis are (i) AuNPs used in such studies need not be surface-modified, (ii) Aptamers need not be labelled (which might interfere with target binding), (iii) Signal is a rapid visual colour transformation and (iv) Assay can be carried out in aqueous solution.

In one study (Li et al., 2009), heavy metal (Hg^{2+}) was detected in water samples using this principle. Aptamers specific to mercury are rich in thymine bases, since mercury as such tends to form thymine–mercury ions–thymine bond (T–Hg^{2+}–T) with its aptamer. This interaction is more specific than that of aptamer with AuNPs. In presence of mercury ions, AuNPs are left unprotected in solution. As a result, NaCl in the solution can screen the electrostatic repulsive forces around AuNPs and make them susceptible to aggregation, thereby turning the colour of the solution to purple. The assay could detect mercury ions over a wide (five orders of magnitude) linear range, with the lowest sensitivity reported till then (1×10^{-4}–1×10^{-9} M, 1 nM). Owing to the high selectivity of thymine for Hg^{2+}, as compared to other metal ions, this principle has been exploited in several other formats of mercury ion sensing (discussed later).

Colorimetric aptasensing has been used to detect several antibiotics in food samples. Many of these reports include selection of aptamers for a given target. Analyte binding in these systems was based on weak intermolecular binding forces between aptamer and analyte (and not on complexation of bases with the target as in the case of Hg^{2+}). An example is oxytetracycline (OTC) sensor developed by Kim et al. (2010). RNA aptamers are less stable when compared to DNA aptamers hence, they need to be functionalized to make them stable and suitable for use as recognition elements in sensors. One such study involved 2′-fluoro-pyrimidine derivatization of RNA aptamer for reliable detection of aminoglycosides (Derbyshire et al., 2012). Various food analytes and contaminants such as ochratoxin A (OTA) (Yang et al., 2011), acetamiprid (Shi et al., 2013), bisphenol-A (Mei et al., 2013; Ragavan et al., 2013), theophylline (Katiyar et al., 2013), melamine (Yun et al., 2014) etc. were detected using the same principle of 'non-crosslinking

aggregation' mechanism of AuNPs. (Table 1).

A slightly different aggregation-based indirect colorimetric approach was carried out by Wu et al. (2012a) for heavy metal detection. In their study, the aptamer did not adsorb on AuNP surface; rather it formed a duplex with a cationic polymer in the absence of analyte. The cationic polymer (poly(diallyldimethylammonium) abbreviated as PDDA), in unbound state, possesses the ability to aggregate AuNPs. On addition of analyte, the aptamer more specifically binds to it, releasing the polymer and in turn aggregating the nanoparticles. The group applied the technique for highly selective detection of As^{3+} with a detection limit of 5.3 parts per billion (ppb).

Detection of tetracycline (TET) in milk and aqueous solutions was reported by He and coworkers using two different principles – one being cationic polymer based approach (He et al. 2013a) similar to the aforementioned work of Wu et al. (2012a) for arsenic detection. Tetracycline could be detected visually at a limit of 1 μM and up to 45.8 nM by the colorimetric detector, using PDDA. The biosensor exhibited high selectivity over other antibiotics and very good recovery in milk. The other approach, published two days before the aforementioned, used cetyltrimethylammonium bromide (CTAB) to bind to the same aptamer, and excess of NaCl to aid in aggregation (He et al., 2013b). However, the principles are very different. In the second case, the aptamers were able to protect the AuNPs even after binding to the analyte. The unbound CTAB and excess NaCl could not aggregate AuNPs and thus analyte introduction led to colour change from blue to red. The reason for the inability of aptamer–analyte complex to protect AuNPs in presence of PDDA in the first strategy remains unexplained.

The principle of protection of gold nanoparticles by aptamers, though commonly applied, suffers from certain drawbacks. For practical purposes, there is often a need for separation of unmodified AuNPs or surplus aptamers from the reaction mixture. For large aptamers and comparatively smaller analyte molecules, the aptamer may protect the AuNPs even in the bound form, leading to false negative results. Similar contradiction in protection mechanism exists for polymer-protected NPs, as discussed earlier. To ensure accuracy in experimental results, the exact principle should be proved, for which structural changes and binding events that occur for aptamer, analyte and nanoparticles need to be precisely determined.

A silver reduction based colorimetric sensing technique was proposed by Wang, W., et al. (2011). Here the assay was not dependent on AuNP aggregation; rather on its catalytic property. Poly(dimethylsiloxane) (PDMS)–AuNPs composite film was used as a platform for immobilizing target-specific aptamer. Silver lactate was added onto the film. PDMS–AuNPs–aptamer complex could not reduce silver, since negatively charged unbound aptamers repelled silver lactate, and aptamers completely covered AuNP surface, thereby inhibiting its catalytic effect. Conjugation of target molecules to the modified nanoparticle surface, altered aptamer configuration and its surface charge, increasing the catalytic efficiency of AuNPs for silver reduction and producing a dark colour. The darkness density of silver reduction was used as the marker for quantitative measurement of lysozyme and adenosine 5′-triphosphate (ATP), in the ranges of 1×10^{-2}–1 μg/mL and 1×10^{-4}–1×10^{3} μg/mL, respectively. The issue with the system was that there was very minute difference in readings with variation in analyte concentrations, however, considerable difference in readings was observed with an increase in time. This behaviour necessitated the reading of signals after a certain period (30 min), and readings were linear only for higher lysozyme concentrations. An improved silver based assay for *Salmonella typhimurium* has recently been reported, where recognition by aptamers and signal enhancement was uncoupled. In the assay, the researchers attached *S. typhimurium* specific aptamer to microtitre plate by avidin–biotin linkage, which acted as a recognition element for bacterial cells. At the same time, a second set of aptamers were conjugated to AuNPs by thiol linkage which bound to the cells captured by aptamers on microtitre plate in sandwich design. Finally a silver enhancer solution was used to elevate the signals and the cells could be quantified at sensitive levels with naked eye (Yuan et al., 2014).

3.1.2. *Fluorimetry based sensors*

Fluorimetry is one of the highly selective and sensitive optical sensing methods in which a molecule/dye/nanomaterial emits light while returning to ground state after absorbing higher energy radiation at shorter wavelengths. A few exceptions include upconversion nanoparticles which emit light at a shorter wavelength than the absorbing wavelength (discussed earlier). Most fluorescence based aptasensors use the competitive binding of the analyte and a complementary strand to the aptamer. In presence of the analyte, the aptamer structure changes (structure-switching), and the complementary strand is displaced from the hybridization complex, resulting in a fluorescence signal. Alternatively, a few sensors rely on binding of a fluorescent molecule to the analyte and its subsequent separation using an aptamer. Based on the latter, some reports have been discussed in Section 5 where magnetic nanoparticles are used for separation of aptamer–analyte complex.

A single-QD-based aptasensor was developed for cocaine (Fig. 1) using competitive binding principle. It was capable of sensing the presence of cocaine through both signal-off and signal-on modes. In the 'turn-off' mode, cocaine aptamer was sandwiched between a Cy5-labelled oligonucleotide and a biotinylated oligonucleotide. This sandwich hybrid was then assembled on the surface of a QD (emitting at 605 nm) through biotin–streptavidin binding to form the 605QD/aptamer/Cy5 complex. The structure switching of aptamer on binding of cocaine led to the detachment of a Cy5 bound oligonucleotide, and as a result fluorescence resonance energy transfer (FRET) ceased between QD and Cy5. In the 'turn-on' mode the cocaine aptamer was sandwiched between a 5′-Cy5-labelled and 3′-biotinylated oligonucleotide and an Iowa Black RQ-labelled oligonucleotide. Even if FRET occurred between 605QD and Cy5, the Cy5 fluorescence was quenched by the nearby Iowa Black RQ, keeping the sensor in the signal-off state. Addition of cocaine to the sensor induced the release of the dye-labelled oligonucleotide from the complex and turned the fluorescence on (Zhang and Johnson, 2009).

Similar FRET-based signal 'turn-on' sensors were developed for OTA by Sheng et al. (2011), Guo et al. (2011) and Duan et al. (2012a). All three systems used carboxyfluorescein (FAM) – tagged ssDNA aptamers as the fluorophore, and 'super quencher' graphene oxide (GO), single-walled CNTs and AuNPs respectively, as quenchers. Poly(vinyl pyrrolidone) (PVP) was used in the assay, in order to avoid non-specific adsorption of OTA on GO surface. Addition of PVP helped in decreasing the detection limit of OTA from 21.8 to 18.7 nM. Multiplexed detection of mycotoxins in solution was achieved by using multicolour UCNPs as fluorophores and GO as quencher (Wu, S., et al., 2012) (Fig. 3), where OTA and Fumonisin B1 aptamers were tagged to the UCNPs via avidin–biotin linkage. GO was used as quencher for detection of proteins (lysozyme, cytochrome c and thrombin) using FAM labelled aptamers. The three different aptamer–protein complexes were separated by an isoelectric focusing-capillary zone electrophoresis based microfluidic system (Lin et al., 2014).

Such sensors are accurate and give linear resolution over a wide range, however, when assays are carried out in solution, it is often required to separate the quencher from the fluorophore molecule. This is because even after detachment of the complementary strand its signals tend to be quenched due to proximity in solution

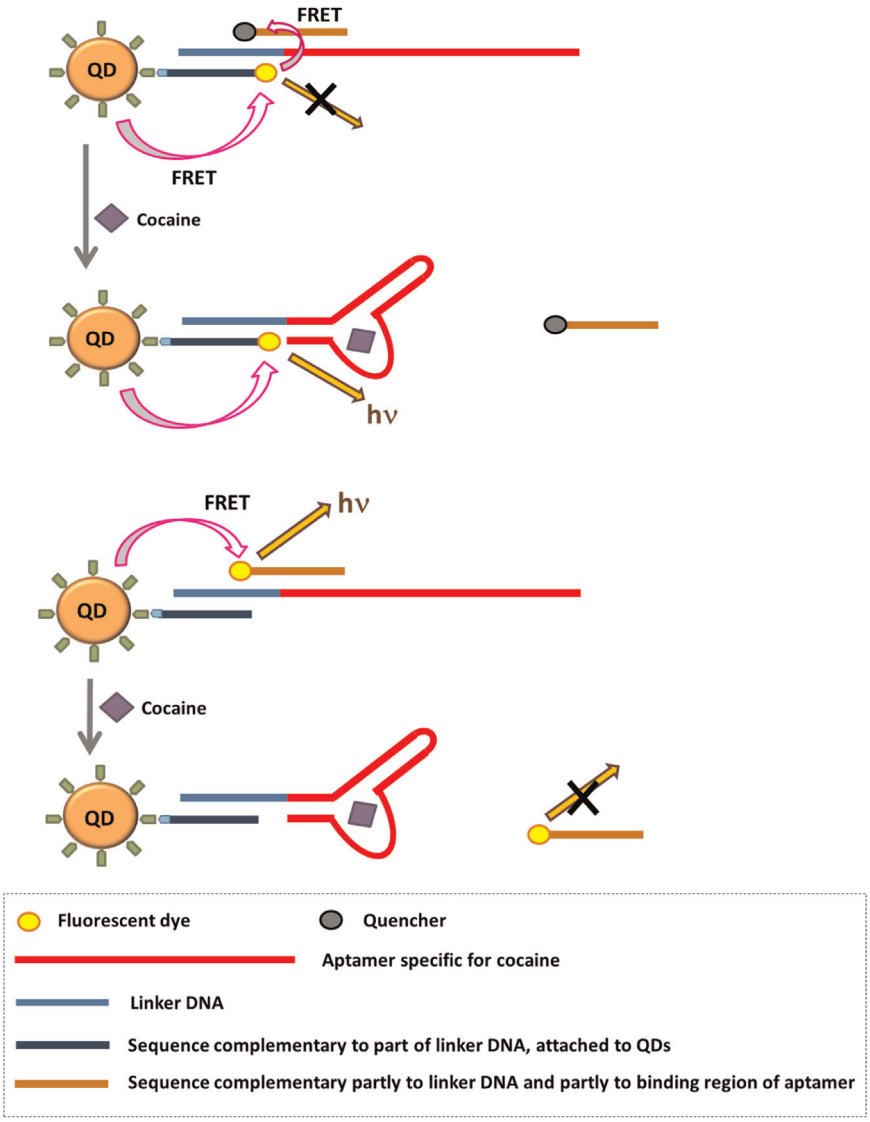

Fig. 1. (a) Signal-on sensor design for cocaine: In the absence of cocaine, Cy5 dye fluorescence (due to FRET between QD and Cy5 dye) was quenched by Iowa Black RQ (a quencher). Presence of cocaine led to the formation of a cocaine–aptamer complex, releasing the quencher-bound oligonucleotide, due to which the dye fluorescence was activated. Signal-off sensor: When cocaine was absent, fluorescence could be observed due to FRET between QD and Cy5 dye. In presence of cocaine, cocaine–aptamer complex was formed, with release of dye-bound oligonucleotide and the subsequent abolishment of FRET between QD and Cy5. Thus fluorescence was turned off.

and thus sensitivity is compromised. Tagging aptamers is also a challenge as it might hinder analyte binding.

An interesting biosensing technique was developed for the determination of cocaine based on the principle of rolling circle amplification (Fig. 2). Here, cocaine aptamers immobilized onto AuNPs, were attached to magnetic beads. The complementary DNA strand was then allowed to hybridize with the aptamer. The presence of cocaine induced competitive displacement of the complementary strand from the aptamer. The aptamer-magnetic beads were subsequently subjected to magnetic separation. The remaining short strands were then used as primers to initiate rolling circle amplification. Molecular beacons hybridized with the end products of the amplification generated fluorescence signals. Though the technique required several major steps (release of short strand, separation of short strand, DNA amplification and molecular beacon hybridization), the advantage was that the separation of aptamer–cocaine complex by magnetic beads reduced the background signal and rolling circle amplification enhanced assay signal, enabling detection of cocaine, as low as 0.48 nM (Ma et al., 2011).

To avert the issue of background quenching due to the presence of fluorophore and quencher in same solution, strip-based sensors were developed. Wang et al. (2011a) demonstrated a fluorescent strip aptasensor for the sensitive and rapid on-site detection of OTA in red wine samples. They used QD-tagged aptamer specific to OTA as the capture agent along with two more probe sequences, in which probe-1 was complementary to the aptamer sequence and probe-2 had only thymine (T) bases in it. Probe-1 and probe-2 spotted on the strip served as test and control lines separately. Absence of OTA in test samples was indicated by the fluorescent test line due to the hybridization of aptamer and probe-1, however, if aptamer bound with OTA, it did not fluoresce due to inability to hybridize with probe-1. The same group later used AuNPs instead of QDs as colour indicator in a chromatographic strip sensor for OTA (Wang et al., 2011b). Recently, Bruno (2014) undertook a comparative study of the sensitivities of pathogen detection by lateral flow (LF) test strips using QD–DNA aptamer conjugate and those using AuNPs. Aptamers recognizing *Escherichia coli*, *Listeria monocytogenes* and *Salmonella enterica* were paired as capture and reporter probes to assess which yielded the most sensitive detection of their analyte bacteria using a colloidal gold screening system. The visible limit of detection (LOD) for the

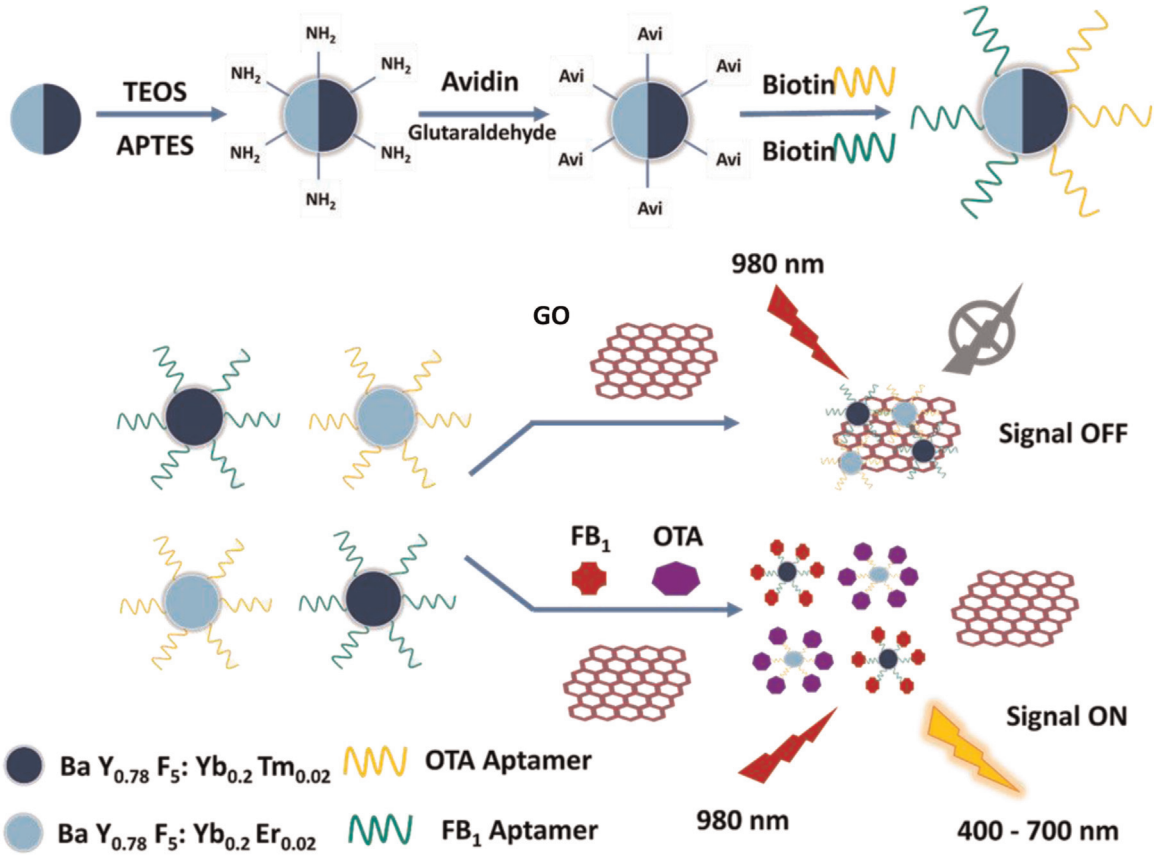

Fig. 3. Multiplexed upconversion (UC) FRET between aptamers–UC nanoparticles (UCNPs) and graphene oxide (GO) for FB1 and OTA detection: In absence of analytes the UCNPs bind to GO, which quenches their signals. In presence of analyte, UCNPs are unable to bind to GO, signal remains on.

best *E. coli* aptamer-LF system was ~6000 *E. coli* O157:H7 and ~3000 *E. coli* 8739 in buffer. These LODs could be reduced to ~300–600 bacterial cells per test respectively by using the QD–aptamer strip system. For capture, a novel dual biotin/digoxigenin-end labelled aptamer was linked to streptavidin-colloidal gold or QDs which bound to anti-digoxigenin antibody control line. Strip-based sensors involve multiple immobilization steps, but they provide the benefit of on-field monitoring and portability.

Another approach to evade quenching in solution is to immobilize any one component to a solid support, which facilitates separation of the counterpart. A real-time flow sensor was developed by Bogomolova and Aldissi (2011). Here, also, the QD-tagged complementary oligonucleotide detached from the DNA aptamer upon binding with the analyte, but the difference was that the aptamer was immobilized to a support and was not tagged to any quencher. The bound QD–oligonucleotide showed fluorescence. On attachment of analyte, the oligonucleotide was released and washed away, leading to decrease in fluorescence. The prototype developed was tested for ATP detection in biological buffer where the LOD was found to be 0.1 mM. The developed sensor was portable and easy to use with scope of further miniaturization, multiplexing and biological pathogen detection.

Single oligonucleotide based molecular beacons have been used to detect Hg^{2+} (Tan et al., 2013). In this format the fluorophore and the quencher are attached to either ends of the same aptamer molecule. On analyte binding and subsequent aptamer configuration change, the ends might come closer or move apart, either quenching the fluorescence or restoring it. In the mentioned report the fluorophore used was FAM, while the quencher being AuNPs. The technique is simpler than formats discussed earlier, as it does not require a second oligonucleotide or a hybridization step and does not pose an issue of background quenching of the fluorophore. However, aptamer structure plays a very important role in this case. The sensor works only for oligonucleotides whose ends are considerably far apart either before or after analyte binding.

Flow cytometry, a high throughput biophysical analytical technique, was employed for quantitative detection of bacterial cells (*Vibrio parahaemolyticus* and *S. typhimurium*) (Duan et al., 2013). In the protocol, two different QDs, one having emission at 535 and the other at 585 nm served as optical labels. They were covalently conjugated with aptamers which were specific to *V. parahaemolyticus* and *S. typhimurium*, respectively. Based on the presence of bacterial cells in the samples, the aptamers specifically bound to them and the respective emission signals corresponded to the number of cells present. Recently, synthesis of DNA-scaffolded silver nanoclusters (AgNCs) was used for the first time to design a fluorescent sensor for OTA. OTA aptamers along with a complementary strand were conjugated to magnetic beads. After OTA bound to aptamers, the complementary strand was detached and magnetically separated from the reaction mixture. This short strand served as a template for the formation of silver NCs, which fluoresce at 632 nm (Chen et al., 2014).

3.1.3. Chemiluminescence based sensors

Chemiluminescence (CL) is the emission of light from a chemical reaction in which an intermediate chemical compound emits photons while returning to ground state from excited electronic state. CL reactions are generally multi-step oxidation reactions with fast reaction kinetics and find huge applications in biosensing due to their advantages such as wide linear range, good sensitivity, operational simplicity, short assay time and relatively low cost compared to chromatographic techniques. CL sensors coupled with nanoparticles have been studied extensively in

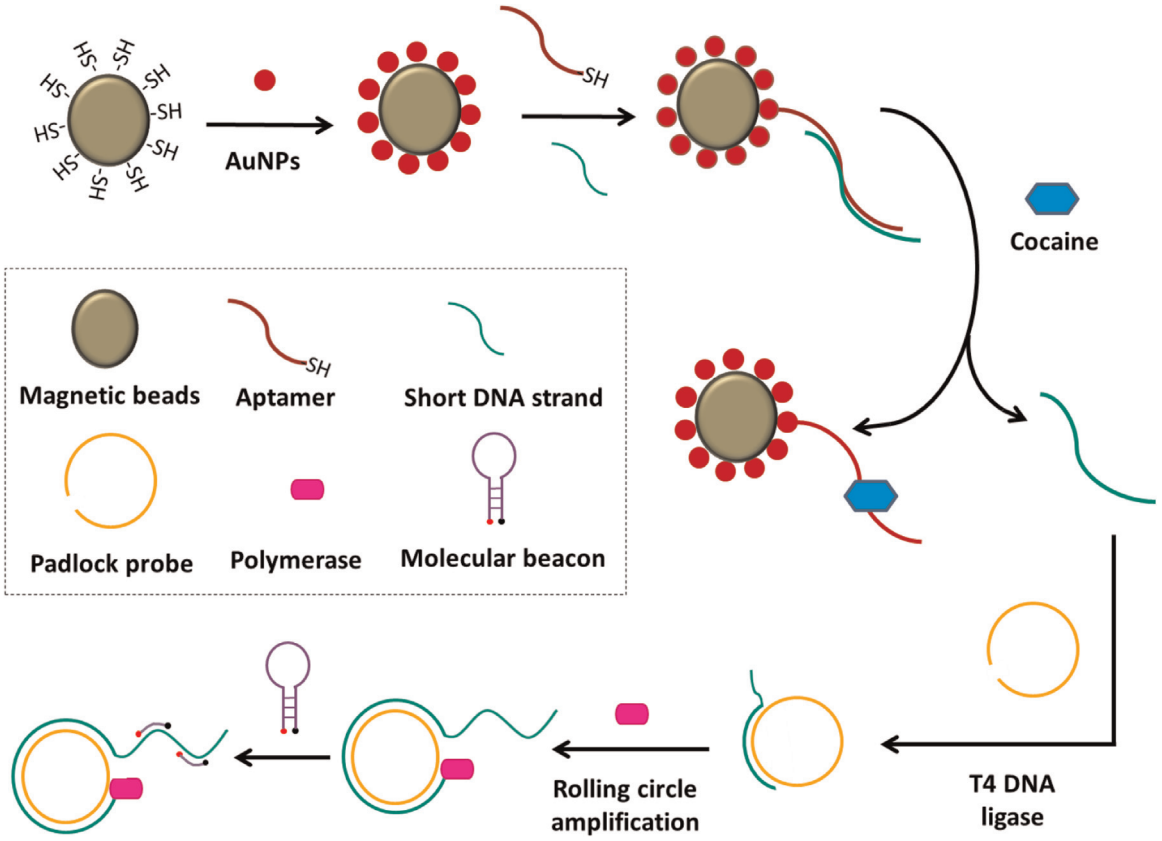

Fig. 2. Fluorescence biosensor to detect cocaine: The detection is based on signal amplification by gold nanoparticles under rolling circle amplification and the separation by magnetic beads which reduces the background signal.

recent times (Giokas et al., 2010; Li et al., 2014).

CL can be coupled to electron generation, with advantages such as control over the intensity and course of light production, minimal requirement of reagents for immobilization on electrodes and regeneration of reactants. An electrochemiluminescent aptamer biosensor for OTA detection in naturally contaminated wheat samples was fabricated by immobilizing complementary DNA sequence of OTA aptamer onto the surface of an AuNP-modified gold electrode. *N*-(4-aminobutyl)-*N*-ethyl-isoluminol (ABEI)-labelled aptamer that served as the electrochemiluminescent probe, was hybridized to the above DNA. Hydrogen peroxide was used to co-oxidize ABEI. In presence of OTA, the electrochemiluminescence (ECL) signal decreased due to the dissociation of ABEI-labelled aptamer from electrode-attached DNA strand. This set-up involved signal amplification by both AuNPs that catalyze the CL, and H_2O_2 that increases rate of oxidation of ABEI, lowering the LOD to 0.007 ng/mL (Wang et al., 2010).

CL signals can be enhanced also by chemiluminescence resonance energy transfer (CRET) where the emitted light energy is absorbed by a second species that in turn emits at higher intensity or wavelength. Three DNAzyme-catalyzed CL based detection techniques, one each for metal Ions, ATP and target DNA, were developed by Freeman et al. (2011). Aptamer domains against ATP or Hg^{2+}-specific sequences were self-assembled with nucleic acid subunits comprising of fragments of the horseradish peroxidase (HRP)-mimicking DNAzyme. In the presence of ATP or Hg^{2+} the oligonucleotides form active hemin–G-quadruplex DNAzyme structure, which catalyze luminol chemiluminescence. When CdSe/ZnS QDs were attached to one of the aptamer subunits, CRET occurred between the generated chemiluminescence and QDs, producing an enhanced signal. Alternatively, if QDs were attached with a hairpin nucleotide, a 'caged' configuration resulted. The hairpin structure was opened by the target DNA assembling the hemin–G-quadruplex DNAzyme that stimulated the CRET signal. By the application of QDs, of three unique sizes, functionalized with different hairpins, the multiplexed analysis of three DNA targets could be achieved by generating different CRET signals (Fig. 4). Later in the year, Freeman and group reported thrombin detection using the same principle. Detection of ATP through CRET between HRP-CL and QDs was repeated. As an addition, FAM was used as another acceptor for CRET. Surprisingly, despite being a later report, the sensitivity achieved for ATP was reduced from 100 nM (Freeman et al., 2011) to 10 μM (Liu et al., 2011).

CRET between TEX 615 dye-conjugated aptamer and 1,1′-oxalyldiimidazole chemiluminescence (ODI-CL) was used for the detection of *V. parahaemolyticus* (Kwun et al., 2014). The dye–aptamer conjugate, bound to *V. parahaemolyticus*, absorbed light from the ODI-CL reaction and emitted at 615 nm due to CRET. Aptamers which are in excess bound to GO due to π–π interaction, quenching the CRET between TEX 615 dye and ODI-CL reaction. The obtained CL signals were proportional to the amount of *V. parahaemolyticus* cells present in the sample with an LOD of 2230 cells/mL.

3.1.4. *Surface plasmon resonance and Rayleigh scattering based sensors*

SPR sensors, as discussed in Section 3.1.1, are a class of refractometric sensors which measure the properties of electromagnetic waves based on the changes in the refractive index due to any chemical/biological/physical event on the sensor surface (Homola, 2008). The signal generated due to propagating SPR from a noble metal-coated surface is transduced by dedicated SPR sensing instruments. In SPR condition, Rayleigh scattering (re-emitted/scattered photons having same amount of energy as

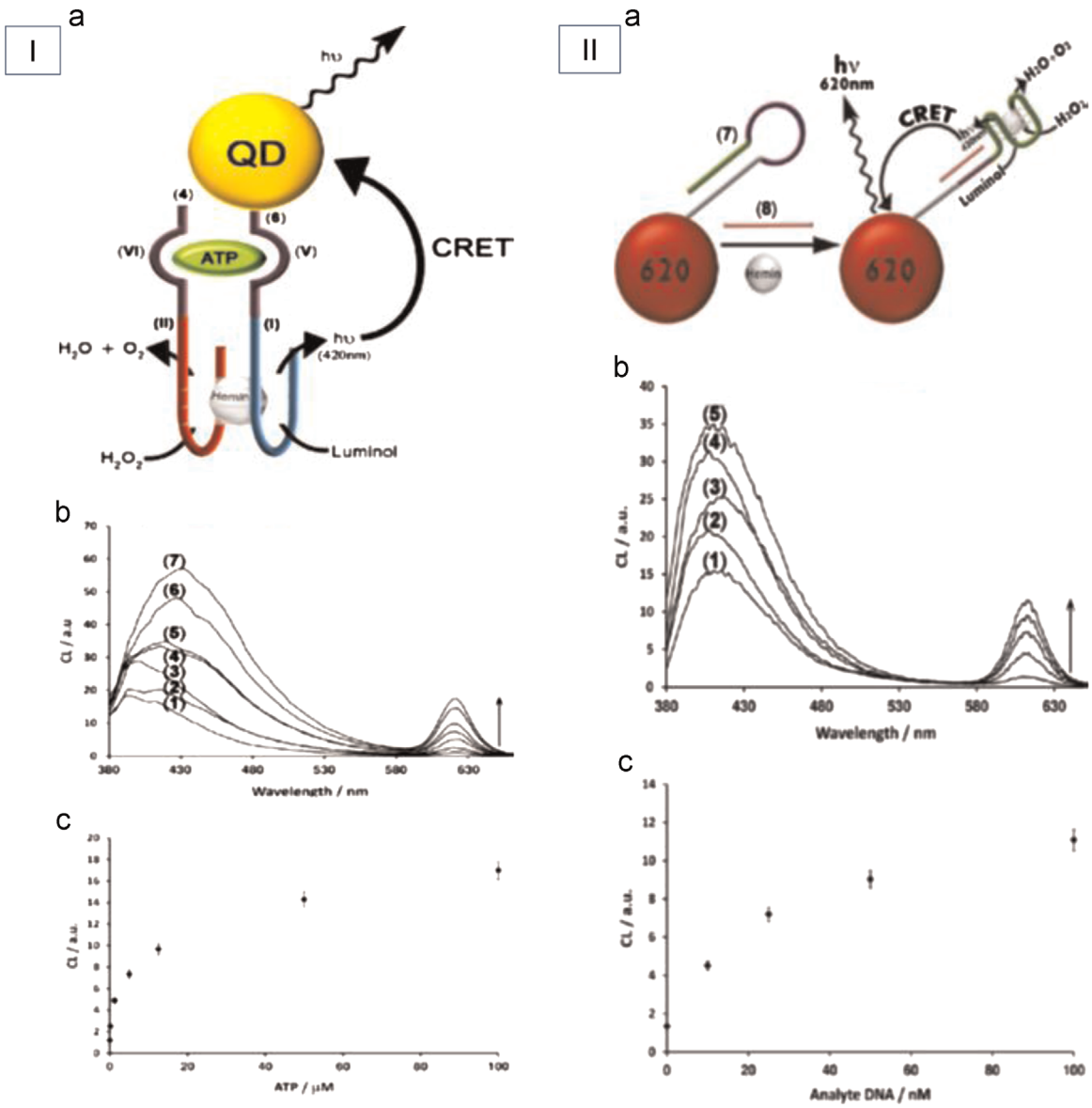

Fig. 4. Analysis of ATP and target DNA through CRET. I (a) Analysis of ATP through CRET from luminol, oxidized by the assembled hemin G-quadruplex, to the QDs. (b) Luminescence spectrum for the CRET signal of QDs at λ=612 nm in absence of ATP, curve (1), and in presence of different concentrations of ATP: (2)–(7) (c) Calibration curve for the increase in the CRET signal at λ=620 nm. II (a) Analysis of target DNA through CRET. (b) Luminescence signal spectrum for CRET signal of the QDs at λ=620 nm in the absence of DNA (8), curve (1), and in the presence of different concentrations of (8): (2)–(5) (c) Calibration curve corresponding to the increase in the CRET signal at λ=610 nm. [Reprinted from Freeman et al. (2011) with permission from ACS publishing.]

absorbed incident photons) is also found to be maximum and the phenomenon is denoted as Resonance Rayleigh Scattering (RRS). The assay mechanism for RRS is the same as localized SPR – in the absence of protecting aptamers, NPs are aggregated with the aid of salt. However, the RRS signal from large aggregated particles is usually measured in synchronous mode in a regular spectrofluorometer.

Pelossof et al. (2011) constructed an aptamer–hemin–G-quadruplex based sensor for detection of Hg^{2+}, adenosine monophosphate and DNA molecules. Usually this DNAzyme complex is used for catalysis of redox systems, producing electrochemical or chemiluminescent signals, as reported by the same group (Freeman et al., 2011; Liu et al., 2011). However, in this assay the aptamer was conjugated to AuNPs to amplify SPR signals due to simultaneous formation of hemin–G-quadruplex and analyte binding. The sensor could identify even minute changes in refractive index of the plasmon surface, and mercury ions could be detected to an exceptionally low concentration (10 fM).

An aptamer selected for Ara h1 was utilized for its detection in buffer and food matrix using fibre optic surface plasmon resonance (FO-SPR) biosensor platform. Aptamers were conjugated to the probe tip through streptavidin–biotin linkage to capture Ara h1 from the sample matrix and then the tip was dipped in buffer containing polyclonal antibodies against Ara h1. In order to improve the signals, the tip was again dipped in a solution containing protein A–AuNPs conjugate. Protein A with high affinity to Fc portion of antibody bound with it and induced a shift in wavelength compared to control samples (Tran et al., 2013).

Several gold and silver nanoparticle based detection platforms for food and water contaminants using RRS spectral intensity difference between dispersed and aggregated nanoparticles (NPs) have been demonstrated. The Hg^{2+}–thymine base-pairing principle was used for Hg^{2+} detection by Jiang and coworkers, using four approaches, each with slight modifications. In the first one (Jiang et al., 2009), when aptamers bound to mercury ions, released AuNPs aggregated to form larger particles causing linear

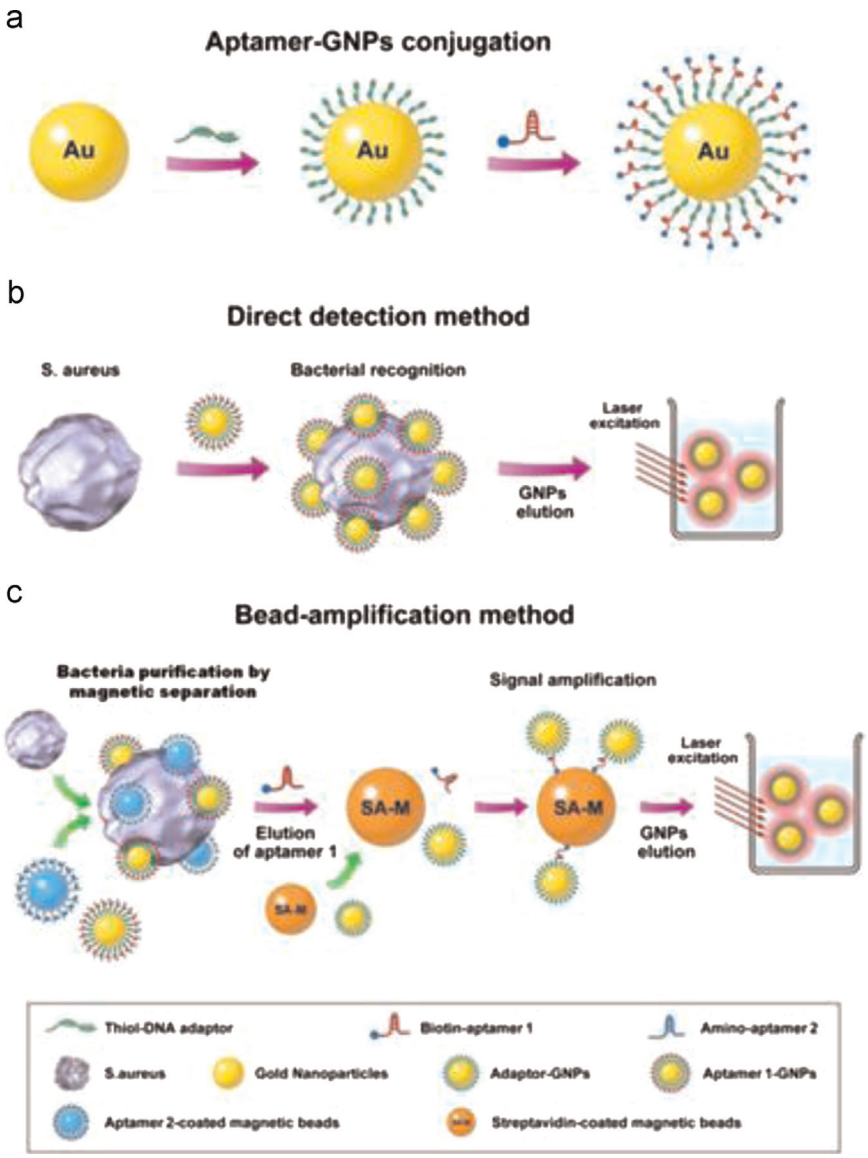

Fig. 5. Detection of single cell of *Staphylococcus aureus* using Resonance Rayleigh Scattering (a), Aptamers conjugated onto AuNPs (referred in the figure as GNPs) with thiol-DNA adaptors. (b) In direct detection method, aptamer–AuNPs were incubated with *Staphylococcus aureus* cells. After removal of unbound aptamer–AuNPs, bound aptamer–AuNPs were eluted and their light-scattering signals analyzed. (c), Bead-based amplification for *Staphylococcus aureus* detection: AuNPs were functionalized with biotin–aptamer 1 and aptamer 2 was conjugated to magnetic beads. Aptamer 1-AuNPs and aptamer 2-magnetic beads interacted with *Staphylococcus aureus*. The resulting complexes were magnetically separated. Bound biotin–aptamer 1 was eluted by heating, followed by further incubation with streptavidin (SA)-coated magnetic beads and excess of reporter-AuNPs (conjugated with DNA adapter). The reporter-AuNPs were then captured with SA-magnetic beads in the presence of biotin–aptamer 1. The bound reporter-AuNPs were eluted with NaOH and their light-scattering signals were analyzed. [Reprinted from Chang et al. (2013) with permission from Nature Publishing Group.]

enhancement of the RS intensity at 540 nm, in a range of 1.3–1667 nM mercury ions, with detection limit of 0.7 nM. Large nanogold particles were removed by membrane filtration to increase sensitivity. The filtrate consisting of excess Au–aptamer exhibited a catalytic effect on the new Cu_2O particle reaction between NH_2OH and Cu^{2+}–ethylenediaminetetraacetic acid (EDTA) complex at 60 °C, producing an RS signal at 602 nm. Detection limit was improved to 0.03 nM. In the second approach, the aggregation of AuNPs was brought about by addition of NaCl, and no catalytic effect of AuNPs was studied (range 0.39–1666.7 nM, detection limit 0.1 nM) (Wen et al., 2010). In the third work, the reduction of $HAuCl_4$ by ascorbic acid was targeted, which appeared as RS peak at 596 nm. In this case the linear range of detection was found to be 0.08–888 μg/mL Hg^{2+}, with detection limit of 0.034 μg/mL (Jiang et al., 2010). In 2011, the fourth work was published where gold–ruthenium NPs were used, aggregation of which induced an increase in the RS signal at 592 nm. The reaction between sodium iodide and sodium chlorate was catalyzed by dispersed NPs and the reaction product I_3^- combined with tetradecyldimethylbenzyl ammonium chloride to produce association particles which exhibited the strongest resonance scattering peak at 472 nm. The response was linear to the concentration of Hg^{2+} in the range 0.0067–3.3 nM (Liang et al., 2011a). This method, though more sensitive than the first two formats, had a higher LOD of 1.5 pM than that achieved in the third approach (LOD 0.17 pM) (Jiang et al., 2010). The authors justified the superiority of their method by claiming that the cost of operation was lower than that for the nanogold–$HAuCl_4$–ascorbic acid system.

Melamine detection was attempted by the same group using melamine aptamer protected silver nanoparticles (AgNPs). However, in this case, addition of melamine did not release the nanoparticles. Instead the analyte interacted through coordinate bonds with NaCl and aptamer–AgNPs to form large aggregated particles leading to considerable increase in the RS intensity (Liang et al.,

2011b). Later in the same year, the authors published their work on RRS detection of melamine in milk using AuNPs instead. Increased RRS intensity was linear to melamine concentration in the range of 1.89–81.98 μg/L and as low as 0.98 μg/L melamine could be detected. Here the researchers incorporated catalytic effect of AuNPs, on the slow Cu_2O particle reaction between Fehling reagent and glucose, achieving higher sensitivity. The catalytic activity was weakened by aggregation, showing a reduced RRS peak intensity at 614 nm (linear range: 0.63–47.30 ng/L melamine, detection limit: 0.38 ng/L) (Liang et al., 2011c). With AgNPs also, the group had earlier worked on Fehling reaction catalysis (Jiang et al., 2011).

Another technique was designed for As^{3+} detection using assembled nanoparticles of different sizes via controlling the concentration of arsenic-binding aptamers in crystal violet solutions. The introduction of As^{3+} changed the size of nanoparticles, causing great variation in the RRS intensity at 310 nm. Using large and small nanoparticles, As^{3+} could be detected at as low as 0.2 ppb concentration with high selectivity over other metal ions (Wu et al., 2012b).

In 2013, Chang et al. detected single cells of *Staphylococcus aureus* using RRS. Two aptamers specific to the pathogen were chosen, designated aptamer 1 and aptamer 2. In the direct detection method the cells were tagged with aptamer 1 functionalized AuNPs, the attached AuNPs were then eluted out and quantified using RRS. In the bead-based amplification (indirect) method, both aptamer 1-coated AuNPs and aptamer 2-coated magnetic beads were allowed to bind to the *Staphylococcus aureus* cells, followed by magnetic separation. Attached aptamer 1 was eluted out and linked to a second set of streptavidin coated magnetic beads, while their free ends remained bound to complementary strand-coated AuNPs. These AuNPs were then eluted out and subjected to light scattering measurement. It was observed that a single cell yielded 10^4 AuNPs, which enabled detection of a cell in 1.5 h itself (Fig. 5).

3.1.5. Surface-enhanced Raman scattering (SERS) and surface-enhanced resonance Raman scattering (SERRS) based sensors

The enhancement of Raman signals by nanoparticles is anticipated to be a prospect for single molecule detection. The innovative spectroscopic technique is termed SERS, and involves conjugation of the biorecognition molecule to a plasmonic substrate e.g. gold or silver nanoparticles (Craig et al., 2013). He et al. (2011) demonstrated an aptamer based SERS assay for the qualitative detection of ricin, classified as a 'bioterror agent', in liquid foods. The aptamer was tagged with silver dendrites through thiol linkage. On capture of the target, a shift in wavelength of the Raman signal was evident. Aptamer conjugated silver dendrites were similarly used for detection of four pesticides (isocarbophos, phorate, omethoate and profenofos). The LODs were 3.4 μM (1 parts per million, ppm), 0.4 μM (0.1 ppm), 24 μM (5 ppm) and 14 μM (5 ppm), respectively (Pang et al., 2014). AuNPs were used as SERS substrates for detection of BPA by Marks et al. (2014). Formation of self-assembled monolayers on the surface of NPs served multiple purposes of nanocolloid stabilization, protection from chemical degradation and specific aptamer conjugation.

Zhang et al. (2013) demonstrated an aptamer based surface-enhanced resonance Raman scattering (SERRS) sensor for the detection of mercury ions at sub-parts per trillion (ppt) levels. Aptamer bound to Cy5 (Cyanine dye) was conjugated to the nanoporous gold surface by thiol linkage which acted as a capture agent for mercury ions and also as optical tags in the assay. In the absence of mercury ions, the Cy5 dye interacted with the gold surface and the Raman signals were high due to localized plasmon enhancement. If mercury ions were present in the sample it bound to the aptamer, releasing Cy5 that moved away from the surface leading to reduced Raman signals.

3.2. Electrochemical biosensors

Electrochemical sensors are the most sought sensing systems in recent times due to their selectivity and real time application in food analysis. Essentially change in current, voltage, potential difference or impedance due to oxidation/ reduction of chemical/ biological molecule is measured with the help of electrodes and an electrochemical unit (Grieshaber et al., 2008; Kimmel et al., 2012). Electrodes are largely modified in order to improve the performance of sensors mostly by conjugation of specific recognition elements such as aptamers, antibodies and receptors of interest. Nanomaterials are incorporated into electrodes to increase their surface area that improves conjugation and to catalyze redox reactions (Walcarius et al., 2013; Chen and Chatterjee, 2013). In the following section, recent advancements in electrochemical aptasensors with respect to food analysis have been discussed.

Several electrochemical aptasensing techniques which were developed prior to 2011 have been reviewed by Yuan et al. (2011) and Radi (2011). Zhu et al. (2009) reported a portable electrochemical sensor for the detection of Hg^{2+} ions in aqueous solution by using T–Hg^{2+}–T bonding with aptamer. The thiolated oligonucleotide probe was immobilized on Au electrodes to capture free Hg^{2+} in aqueous media, which could then be electrochemically reduced to Hg^{+}, giving a signal proportional to Hg^{2+} concentration. This strategy could achieve detection limit of 1 μM. In order to improve the sensitivity, AuNPs were co-modified with the aptamer probe and a linking probe. The latter was complementary to a capture DNA probe, immobilized on the Au electrodes. The signal was amplified by more than 3 orders of magnitude, leading to a lower LOD of 0.5 nM. In several similar studies, AuNPs have been used to increase the surface area for aptamer immobilization, and thus for signal amplification e.g. for detection of copper (Chen et al., 2011) and acetamiprid (Fan et al., 2013). A study carried out by Rivas et al. (2015) demonstrated the use of iridium oxide nanoparticles for coating screen printed carbon electrodes. The aptamers were conjugated to the NPs to achieve highly sensitive impedimetric detection of OTA in wine samples.

Often adsorption of non-specific DNA to the surface of electrodes can lead to false results. Kuang et al. (2010) developed an OTA assay where binding of methylene blue dye to guanine residues in DNA molecules was used to avoid this problem. However, there was a requirement of three DNA strands and multiple steps of conjugation and hybridization. Amine-capped DNA (complementary to one end of OTA aptamer) was immobilized on glassy carbon electrode surface. OTA specific aptamer was hybridized with this DNA. AuNPs-tagged DNA sequence complementary to other end of OTA aptamer was added subsequently. The electrodes were first dipped in analyte and then in methylene blue solution. Presence of methylene blue caused a redox current at the electrode amplified by AuNPs. If OTA was present in the sample, it bound to the aptamer specifically such that the AuNPs-tagged DNA sequence was released from the 3-DNA complex, methylene blue molecules attached to this sequence were removed from the electrode surface resulting in electrochemical signal strength to reduce proportionally to the amount of OTA in solution.

Gold nanoparticles composited with polymers and carbon nanomaterials have been used to increase electrochemical efficiency. Conducting polymer/gold self-assembled nanocomposite was used for kanamycin detection in milk samples. The sensor probe was designed by covalently immobilizing a DNA aptamer for kanamycin onto AuNP-comprised conducting polymer, poly-[2, 5-di-(2-thienyl)-1H-pyrrole-1-(*p*-benzoic acid)] (Zhu et al., 2012). To further improve electron transfer, synergistic effect of multiple

nanocomposite layers, namely, chitosan–AuNPs, graphene–AuNPs and multi-walled carbon nanotubes–cobalt phthalocyanine, was used by Sun et al. (2014) for kanamycin detection. Very recently, an electrochemical aptasensor for bisphenol A (BPA) determination in milk products has been developed, based on gold nanoparticles dotted graphene nanocomposite film modified glassy carbon electrode (Zhou et al., 2014). Ferricyanide electrochemical probe was used to monitor binding of BPA to aptamer.

3.3. Other detection formats

A few reports dealing with polymerase chain reaction (PCR) based detection techniques and concentration of aptamer bound analyte by magnetic nanoparticles are discussed here.

A sandwich aptasensing format for *Campylobacter jejuni* was developed, where two aptamers with the highest affinity for the pathogen were selected, one of which was linked to QDs, the other to magnetic nanoparticles. The assay components adhered to polystyrene cuvettes even after capturing magnetic field was removed, thus greatly reducing background signals. Fluorimetry enabled an LOD of 2.5 colony forming units (cfu) in buffer and 10–250 cfu in different food matrices (Bruno et al., 2009).

Magnetic nanoparticles were used for the sample pre-concentration and separation of OTA. In the assay, γ-Fe_2O_3 nanoparticles were impregnated on the surface of copolymer nanospheres to form magnetic nanospheres. OTA specific aptamers were conjugated with magnetic nanospheres and a strong magnetic field was applied for solid phase extraction of the toxin in wheat samples (Wu, X., et al., 2011). Magnetic nanoparticle and aptamer based solid phase extraction was found to be economical in operation when compared to immuno-affinity techniques. The same principle was later used by Wu, S., et al. (2011) for OTA detection. The biotinylated aptamer was attached to the MNP (recognition and concentration element) and a complementary sequence to the aptamer was conjugated to the UCNPs (highly sensitive labels). In presence of OTA, the complementary sequence gets dissociated from the aptamer, followed by its removal from the solution, thereby decreasing fluorescence intensity (directly proportional to OTA concentration). The LOD was found to be 0.0001 ng/mL. UCNPs alongwith amine functionalized Fe_3O_4 MNPs were also used in developing a fluorescence aptasensor for simultaneous detection of *S. typhimurium* and *Staphylococcus aureus* in water samples (Fig. 6). UCNPs acted as dual colour fluorescent labels whose signals got amplified in the presence of magnetic

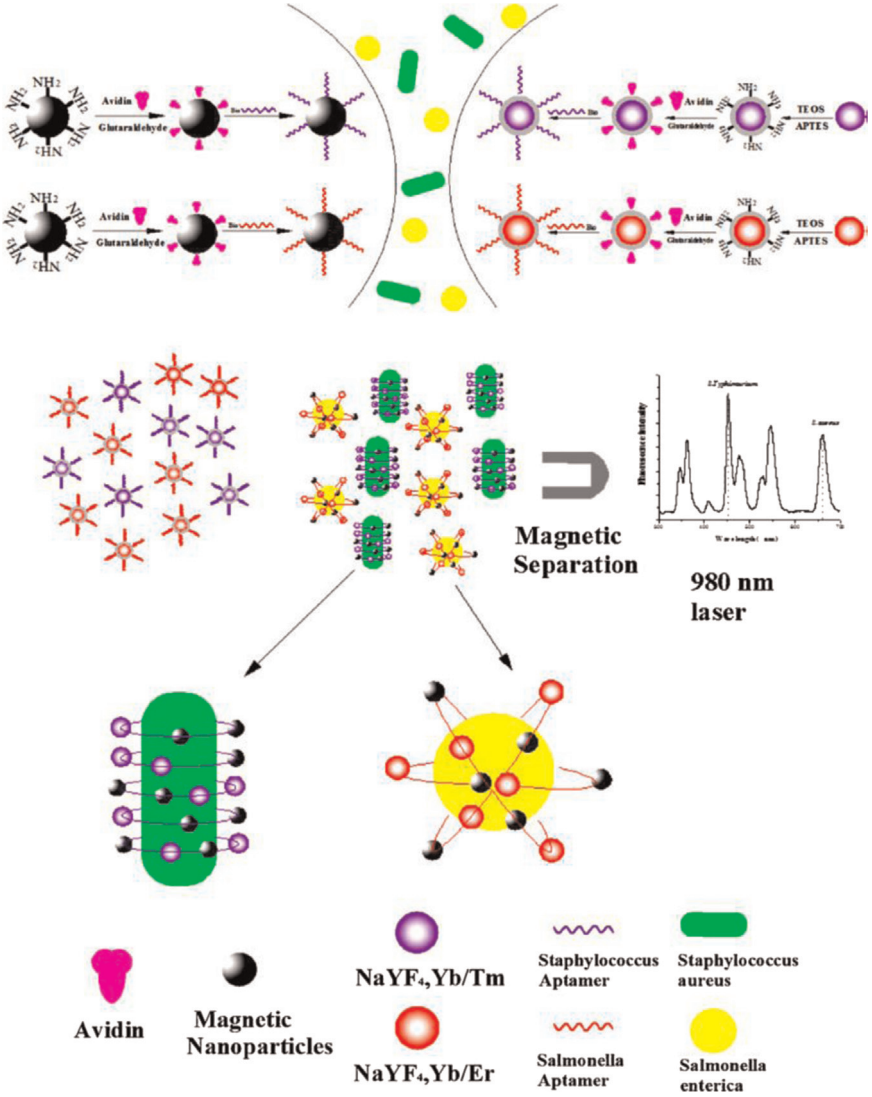

Fig. 6. Simultaneous detection of *Staphylococcus aureus* and *Salmonella typhimurium*: Aptamer-functionalized magnetic nanoparticles and dual-colour upconversion (UC) fluorescence-based bioassay. In presence of analyte both particles bind to the cells. Magnetic nanoparticles aid in separation and UC nanoparticles act as reporters for detection. [Reprinted from Duan et al. (2012b) with permission from Elsevier.]

field which in turn correlated to the number of cells in the sample (Duan et al., 2012b). A similar multiplexed detection of three pathogens was attempted by the same group later (Wu et al., 2014). The UCNPs attached aptamers bound to pathogens in their presence. However, here the assay format was indirect. The excess unbound aptamers hybridized with a second stretch of DNA which were tagged to MNPs. After magnetic separation, luminescence intensity was measured, which was inversely proportional to the number of bacterial cells.

Temur et al. (2012) designed a peptide aptamer modified SERS probe for the detection of Staphylococcal Enterotoxin B (SEB) spiked in milk, blood and urine samples. In the assay, gold nanorods served as Raman label along with DTNB (5,5′-dithiobis-(2-nitrobenzoic acid)) which acted as Raman reporters to generate intense signals. Aptamers were conjugated through thiol bond to the gold coated magnetic rods which acted as capture agents for SEB. They were further separated using a strong magnetic field. The separated SEB aptamer conjugate was mixed with aptamer and DTNB tagged gold nanorods which bound SEB in sandwich fashion. The conjugate enhanced the Raman signals proportional to the amount of SEB available in the sample matrix.

Suh and Jaykus (2013) have reported the selection of aptamers specific towards *L. monocytogenes* using SELEX protocol. As an extension, *L. monocytogenes* specific aptamers were used to design aptamer-magnetic capture-qPCR (quantitative polymerase chain reaction) assay for detection of the pathogen in buffer. The aptamers were conjugated to MNPs and the DNA was isolated from the captured cells for further amplification and quantification using qPCR simultaneously.

4. Conclusions and future perspective

The plenitude of the available literature related to application of aptamers in nanosensors which clearly indicates their successful utilization in several detection formats (a part of it, involving food and water analysis) has been compiled here. As it is evident, the excellent specificity of the aptamers allows a wide variety of analytes, including heavy metal ions, toxins, pathogens, small molecules, nucleic acids and proteins to be detected. Nanoparticles add on to the selectivity and convenience of the diagnostics, by providing larger surface area for aptamer immobilization as well as by conferring their own opto-physical and electrochemical properties to the sensor. However, for a researcher to employ nanoaptasensing in food analysis, it is necessary to prioritize the ultimate aim of the application. For qualitative and semi-quantitative preliminary screening, where sensitivity is not a major concern, fluorescence based assays, coupled to magnetic separation can prove to be useful. In this case, the matrix effect can be minimized by MNPs, followed by fluorimetry. Molecular beacon based fluorescence formats are simple and accurate with linear response, while strip-based and aptamer-immobilized platforms enable removal of background quenching to a large extent, thereby, improving the sensitivity. However, instrumentation is required in this case. To avoid the same, one can use colorimetry, the simplest and fastest visual assay procedure. However, the accuracy of colorimetric methods can only be established once adsorption mechanisms are precisely determined. For extremely toxic compounds and pathogens, more sensitive and accurate methods need to be employed, for example, propagating SPR, Raman spectral techniques and Rayleigh scattering. Though these methods entail use of highly sophisticated dedicated instruments and accurate functionalization procedures, their capability for single molecule detection surpass most bioanalytical techniques. Recent progress in electrochemical techniques have been able to solve many existing issues. Such methods combine the advantages of miniaturization, appreciable sensitivity, accuracy, linearity and simple read-out.

Notwithstanding the enormity of the research in this field, there exists a lot of scope for further investigation. Aptamers have been developed against food contaminants such as Lupan 1 (Nadal et al., 2012), botulinum neurotoxin (Chang et al., 2010), saxitoxin (Handy et al., 2013) and fumonisin B1 (McKeague et al., 2010) which can be used for biosensing in future. There also exists a scope of incorporation of nanoparticles in already existing aptamer based sensor designs for target analytes such as aflatoxin B1 (Shim et al., 2014), endotoxins (Su et al., 2012) and lead ions (Xiang et al., 2009), among others. Novel hybrid nanoparticles such as graphene oxide/nanoclusters (Yin et al., 2013; Liu, X., et al., 2013), polymer/gold nanofilms (Ferrier et al., 2014), ZnO nanoparticle–carbon nanotube–graphene hybrid (Nayak et al., 2013) can be used in aptasensors due to their excellent properties that surpass those of many of the existing nanomaterials. Molecularly imprinted polymeric nanoparticles (polymeric structures build around target molecules to form cavities that can reversibly bind to them) and aptamers have been integrated to combine the specificity and advantages of both (Poma et al., 2015). Such systems can be extended into bioanalysis. Magnetic nanoparticles can be effectively used for separation of target compounds, further improving detection sensitivity. Further, cost-effective aptamer–nanomaterial based kits can be developed for food analysis.

Some obstacles still exist in the development of field-applicable aptasensing techniques. Some of these techniques have specificity dependence on sample conditions such as pH, ionic strength and viscosity, nonspecific interactions of aptamer with the sample matrix and difficulty in selection and development of aptamer against small molecules. As such, in most sensors described here, real sample detection is achieved either by sample pre-treatment or separation of aptamer–analyte conjugate. In other cases, the analysis has been carried out in buffer, with prospective future application in real samples. There exists a need to simplify such pre-treatment procedures. Efforts are now being directed towards improvement of selection techniques to obtain functional and high-affinity aptamers for several small molecular weight analytes. However much sensitive the assay format may be, specificity, which is a major concern both in health and food safety, can only be achieved by selection of narrow range of conditions for SELEX. Also, for on-field monitoring and wide application of aptasensors in food quality assessment, the extremely high cost and difficulty in aptamer functionalization has to be reduced. It can be hoped that further insight into the probable solutions to these problems and in development of novel nanomaterials will boost designing of affordable and easily operable nanomaterial–aptamer based sensing systems. Even if some of these aspects are addressed by the researchers in this area around the world, the objective of this review is considered fulfilled.

Acknowledgements

The authors thank the Director of the CSIR-CFTRI for constant encouragement. RS and KVR are thankful to the Council of Scientific and Industrial Research for providing CSIR-GATE Fellowship. We are grateful to NPMASS-ADA programme of Defence Research and Development Organization (DRDO) for funding related research.

References

Bogomolova, A., Aldissi, M., 2011. Biosens. Bioelectron. 26, 4099–4103.
Bruno, J.G., Phillips, T., Carrillo, M.P., Crowell, R., 2009. J. Fluoresc. 19, 427–435.

Bruno, J.G., 2014. Pathogens 3, 341–355.
Burris, K.P., Stewart Jr., C.N., 2012. Trends Food Sci. Technol. 28, 143–152.
Campas, M., Gariboa, D., Prieto-Simon, B., 2012. Analyst 137, 1055–1067.
Cao, M., Li, Z., Wang, J., Ge, W., Yue, T., Li, R., Colvin, V.L., Yu, W.W., 2012. Trends Food Sci. Technol. 27, 47–56.
Chang, T.W., Blank, M., Janardhanan, P., Singh, B.R., Mello, C., Blind, W., Cai, S., 2010. Biochem. Biophys. Res. Commun. 396, 854–860.
Chang, Y.C., Yang, C.Y., Sun, R.L., Cheng, Y.F., Kao, W.C., Yang, P.C., 2013. Sci. Rep. 3 (1863), 1–7.
Chen, A., Chatterjee, S., 2013. Chem. Soc. Rev. 42, 5425–5438.
Chen, J., Zhang, X., Cai, S., Wu, D., Chen, M., Wang, S., Zhang, J., 2014. Biosens. Bioelectron. 57, 226–231.
Chen, Z., Li, L., Mu, X., Zhao, H., Guo, L., 2011. Talanta 85, 730–735.
Cho, E.J., Lee, J.W., Ellington, A.D., 2009. Annu. Rev. Anal. Chem. 2, 241–264.
Craig, A.P., Franca, A.S., Irudayaraj, J., 2013. Annu. Rev. Food Sci. Technol. 4, 369–380.
Derbyshire, N., White, S.J., Bunka, D.H., Song, L., Stead, S., Tarbin, J., Sharman, M., Zhou, D., Stockley, P.G., 2012. Anal. Chem. 84, 6595–6602.
Dong, Y., Xu, Y., Yong, W., Chu, X., Wang, D., 2013. Crit. Rev. Food Sci. Nutr. 54, 1548–1561.
Duan, N., Wu, S., Ma, X., Chen, X., Huang, Y., Wang, Z., 2012a. Anal. Lett. 45, 714–723.
Duan, N., Wu, S., Yu, Y., Ma, X., Xia, Y., Chen, X., Huang, Y., Wang, Z., 2013. Anal. Chim. Acta 804, 151–158.
Duan, N., Wu, S., Zhu, C., Ma, X., Wang, Z., Yu, Y., Jiang, Y., 2012b. Anal. Chim. Acta 723, 1–6.
Fan, L., Zhao, G., Shi, H., Liu, M., Li, Z., 2013. Biosens. Bioelectron. 43, 12–18.
Ferrier Jr., R.C., Lee, H.S., Hore, M.J.A., Caporizzo, M., Eckmann, D.M., Composto, R.J., 2014. Langmuir 30, 1906–1914.
Freeman, R., Liu, X., Willner, I., 2011. J. Am. Chem. Soc. 133, 11597–11604.
Gill, R., Zayats, M., Willner, I., 2008. Angew. Chem. Int. Ed. 47, 7602–7625.
Giokas, D.L., Vlessidis, A.G., Tsogas, G.Z., Evmiridis, N.P., 2010. Trends Anal. Chem. 29, 1113–1126.
Grieshaber, D., MacKenzie, R., Voros, J., Reimhul, E., 2008. Sensors 8, 1400–1458.
Guo, S., Dong, S., 2011. J. Mater. Chem. 21, 18503–18516.
Guo, Z., Ren, J., Wang, J., Wang, E., 2011. Talanta 85, 2517–2521.
Handy, S.M., Yakes, B.J., DeGrasse, J.A., Campbell, K., Elliott, C.T., Kanyuck, K.M., DeGrasse, S.L., 2013. Toxicon 61, 30–37.
He, L., Lamont, E., Veeregowda, B., Sreevatsan, S., Haynes, C.L., Diez-Gonzaleza, F., Labuza, T.P., 2011. Chem. Sci. 2, 1579–1582.
He, L., Luo, Y., Zhi, W., Zhou, P., 2013a. Food Anal. Methods 6, 1704–1711.
He, L., Luo, Y., Zhi, W., Wu, Y., Zhou, P., 2013b. Aust. J. Chem. 66, 485–490.
Homola, J., 2008. Chem. Rev. 108, 462–493.
Hong, P., Li, W., Li, J., 2012. Sensors 12, 1181–1193.
Iliuk, A.B., Hu, L., Tao, W.A., 2011. Anal. Chem. 83, 4440–4452.
Jariwala, D., Sangwan, V.K., Lauhon, L.J., Marks, T.J., Hersam, M.C., 2013. Chem. Soc. Rev. 42, 2824–2860.
Jiang, Z.L., Fan, Y.Y., Chen, M.L., Liang, A.H., Liao, X.J., Wen, G.Q., Shen, X.C., He, X.C., Pan, H.C., Jiang, H.S., 2009. Anal. Chem. 81, 5439–5445.
Jiang, Z.L., Wen, G.Q., Fan, Y.Y., Jiang, C.N., Liu, Q.Y., Huang, Z., Liang, A.H., 2010. Talanta 80, 1287–1291.
Jiang, Z.L., Zhou, L., Liang, A.H., 2011. Chem. Commun. 47, 3162–3164.
Karkkainen, R.M., Drasbek, M.R., McDowall, I., Smith, C.J., Young, N.W.G., Bonwick, G.A., 2011. Int. J. Food Sci. Technol. 46, 445–454.
Katiyar, N., Selvakumar, L.S., Patra, S., Thakur, M.S., 2013. Anal. Methods 5, 653–659.
Kim, Y.S., Kim, J.H., Kim, I.A., Lee, S.J., Jurng, J., Gu, M.B., 2010. Biosens. Bioelectron. 26, 1644–1649.
Kimmel, D.W., LeBlanc, G., Meschievitz, M.E., Cliffel, D.E., 2012. Anal. Chem. 84, 685–707.
Klug, S.J., Famulok, M., 1994. Mol. Biol. Rep. 20, 97–107.
Kochmann, S., Hirsch, T., Wolfbeis, O.S., 2012. Trends Anal. Chem. 39, 87–113.
Kuang, H., Chen, W., Xu, D., Xu, L., Zhu, Y., Liu, L., Chu, H., Peng, C., Xu, C., Zhu, S., 2010. Biosens. Bioelectron. 26, 710–716.
Kwun, J., Yun, S., Park, L., Lee, J.H., 2014. Talanta 119, 262–267.
Li, L., Li, B., Qi, Y., Jin, Y., 2009. Anal. Bioanal. Chem. 393, 2051–2057.
Li, N., Liu, D., Cui, H., 2014. Anal. Bioanal. Chem. 406, 5561–5571.
Liang, A., Zhang, J., Cai, W., Jiang, W., Li, T., Yao, J., Shang, G., 2011a. Anal. Lett. 44, 1442–1453.
Liang, A., Zhou, L., Jiang, Z., 2011b. Plasmonics 6, 387–392.
Liang, A., Zhou, L., Qin, H., Zhang, Y., Ouyang, H., Jiang, Z., 2011c. J. Fluoresc. 21, 1907–1912.
Lin, F., Zhao, X., Wang, J., Yu, S., Deng, Y., Geng, L., Li, H., 2014. Analyst 139, 2890–2895.
Liu, Y., Zhao, Y., Sun, B., Chen, C., 2013. Acc. Chem. Res. 46, 702–713.
Liu, X., Freeman, R., Golub, E., Willner, I., 2011. ACS Nano 5, 7648–7655.
Liu, X., Wang, F., Aizen, R., Yehezkeli, O., Willner, I., 2013. J. Am. Chem. Soc. 135, 11832–11839.
Luo, F., Zheng, L., Chen, S., Cai, Q., Lin, Z., Qiu, B., Chen, G., 2012. Chem. Commun. 48, 6387–6389.
Ma, C., Wang, W., Yang, Q., Shi, C., Cao, L., 2011. Biosens. Bioelectron. 26, 3309–3312.
Marks, H.L., Pishko, M.V., Jackson, G.W., Cote, G.L., 2014. Anal. Chem. 86, 11614–11619.
Mayer, G., 2009. Angew. Chem. Int. Ed. 48, 2672–2689.
McDonagh, C., Burke, C.S., MacCraith, B.D., 2008. Chem. Rev. 108, 400–422.
McKeague, M., Giamberardino, A., DeRosa, M.C., 2011. Advances in aptamer-based biosensors for food safety. In: Somerset, V. (Ed.), Environmental Biosensors. Intech Publishers, Rijeka, Croatia, pp. 17–42.
McKeague, M., Bradley, C.R., Girolamo, A.R., Visconti, A., Miller, J.D., DeRosa, M.C., 2010. Int. J. Mol. Sci. 11, 4864–4881.
Mehta, J., Dorst, B.V., Devriese, L., Rouah-Martin, E., Bekaert, K., Somers, K., Somers, V., Scippo, M.L., Blust, R., Robbens, J., 2011. The use of phages and aptamers as alternatives to antibodies in medical and food diagnostics. In: Komorowska, M. A., Olsztynska-Janus, S. (Eds.), Biomedical Engineering, Trends, Research and Technologies. Intech Publishers, Rijeka, Croatia, pp. 445–468.
Mei, Z., Chu, H., Chen, W., Xue, F., Liu, J., Xu, H., Zhang, R., Zheng, L., 2013. Biosens. Bioelectron. 39, 26–30.
Nadal, P., Pinto, A., Svobodova, M., Canela, N., O'Sullivan, C.K., 2012. PLoS One 7, e35253.
Najafi, M., Khalilzadeh, M.A., Karimi-Maleh, H., 2014. Food Chem. 158, 125–131.
Nayak, P., Anbarasan, B., Ramaprabhu, S., 2013. J. Phys. Chem. C 117, 13202–13209.
Pang, S., Labuzab, T.P., He, L., 2014. Analyst 139, 1895–1901.
Poma, A., Brahmbhatt, H., Pendergraff, H.M., Watts, J.K., Turner, N.W., 2015. Adv. Mater. 27, 750–758.
Pelossof, G., Tel-Vered, R., Liu, X.-Q., Willner, I., 2011. Chem. Eur. J. 17, 8904–8912.
Pérez-López, B., Merkoçi, A., 2011. Trends Food. Sci. Technol. 22, 625–639.
Abd-Elgawad Radi, "Electrochemical Aptamer-Based Biosensors: Recent Advances and Perspectives,"International Journal of Electrochemistry, vol. 2011, Article ID 863196, 17 pages, 2011. http://dx.doi.org/10.4061/2011/863196.
Radom, F., Jurek, P.M., Mazurek, M.P., Otlewski, J., Jeleń, F., 2013. Biotech. Adv. 31, 1260–1274.
Ragavan, K.V., Selvakumar, L.S., Thakur, M.S., 2013. Chem. Commun. 49, 5960–5962.
Rhouati, A., Yang, C., Hayat, A., Marty, J.L., 2013. Toxins 5, 1988–2008.
Rivas, L., Mayorga-Martinez, C.C., Quesada-González, D., Zamora-Gálvez, A., de la Escosura-Muñiz, A., Merkocl, A., 2015. Anal. Chem. 87, 5167–5172.
Rouah-Martin, E., Mehta, J., van Dorst, B., de Saeger, S., Dubruel, P., Maes, B.U.W., Lemiere, F., Goormaghtigh, E., Daems, D., Herrebout, W., van Hove, F., Blust, R., Robbens, J., 2012. Int. J. Mol. Sci. 13, 17138–17159.
Saha, K., Agasti, S.S., Kim, C., Li, X., Rotello, V.M., 2012. Chem. Rev. 112, 2739–2779.
Sánchez-Pomales, G., Santiago-Rodríguez, L., Cabrera, C.R., 2009. J. Nanosci. Nanotechnol. 4, 2175–2188.
Shang, L., Dong, S., Nienhaus, G.U., 2011. Nano Today 6, 401–418.
Sheng, L., Ren, J., Miao, Y., Wang, J., Wang, E., 2011. Biosens. Bioelectron. 26, 3494–3499.
Shi, H., Zhao, G., Liu, M., Fan, L., Cao, T., 2013. J. Hazard. Mater. 260, 754–761.
Shim, W.B., Mun, H., Joung, H.A., Ofori, J.A., Chung, D.H., Kim, M.G., 2014. Food Control 36, 30–35.
Smuc, T., Ahn, I.Y., Ulrich, H., 2013. J. Pharm. Biomed. Anal. 81–82, 210–217.
Song, K.M., Cho, M., Jo, H., Min, K., Jeon, S.H., Kim, T., Han, M.S., Ku, J.K., Ban, C., 2011. Anal. Biochem. 415, 175–181.
Song, S., Wang, L., Li, J., Zhao, J., Fan, C., 2008. Trends Anal. Chem. 27, 108–117.
Sozer, N., Kokini, J.L., 2009. Trends Biotechnol. 27, 82–89.
Su, W., Lin, M., Lee, H., Cho, M., Choe, W.S., Lee, Y., 2012. Biosens. Bioelectron. 32, 32–36.
Suh, S.H., Jaykus, L.H., 2013. J. Biotechnol. 167, 454–461.
Sun, X., Li, F., Shen, G., Huang, J., Wang, X., 2014. Analyst 139, 299–308.
Tan, D., He, Y., Xing, X., Zhao, Y., Tang, H., Pang, D., 2013. Talanta 113, 26–30.
Temur, E., Zengin, A., Boyacı, I.H., Dudak, F.C., Torul, H., Tamer, U., 2012. Anal. Chem. 84, 10600–10606.
Tran, D.T., Knez, K., Janssen, K.P., Pollet, J., Spasic, D., Lammertyn, J., 2013. Biosens. Bioelectron. 43, 245–251.
Tuerk, C., Gold, L., 1990. Science 249, 505–510.
Valdes, M.G., González, A.C.V., Calzón, J.A.G., Díaz-García, M.E., 2009. Microchim. Acta 166, 1–19.
Viswanathan, S., 2011. Nanomaterials in soil and food analysis. In: Gliński, J., Horabik, J., Lipiec, J. (Eds.), Encyclopedia of Agrophysics. Springer, Dordrech, pp. 499–520.
Walcarius, A., Minteer, S.D., Wang, J., Lin, Y., Merkoçi, A., 2013. J. Mater. Chem. B 1, 4878–4908.
Wang, M., Abbineni, G., Clevenger, A., Mao, C., Xu, S., 2011. Nanomed. Nanotech. Biol. Med. 7, 710–729.
Wang, W., Wu, W.Y., Zhong, X., Wang, W., Miao, Q., Zhu, J.J., 2011. Biosens. Bioelectron. 26, 3110–3114.
Wang, L., Chen, W., Ma, W., Liu, L., Ma, W., Zhao, Y., Zhu, Y., Xu, L., Kuang, H., Xu, C., 2011a. Chem. Commun. 47, 1574–1576.
Wang, L., Ma, W., Chen, W., Liu, L., Ma, W., Zhu, Y., Xu, L., Kuang, H., Xu, C., 2011b. Biosens. Bioelectron. 26, 3059–3062.
Wang, L., Xu, M., Han, L., Zhou, M., Zhu, C., Dong, S., 2012. Anal. Chem. 84, 7301–7307.
Wang, Z., Duan, N., Hun, X., Wu, S., 2010. Anal. Bioanal. Chem. 398, 2125–2132.
Wen, G.Q., Liang, A.H., Fan, Y.Y., Jiang, Z.L., Jiang, C.N., 2010. Plasmonics 5, 1–6.
World Health Organization, Regional Office for South-East Asia, 2015. SEA-NUT-196, URL: ⟨http://www.who.int/iris/handle/10665/160165#sthash.H8ZAUV7M.dpuf⟩.
Wu, S., Duan, N., Ma, X., Xia, Y., Wang, H., Wang, Z., Zhang, Q., 2012. Anal. Chem. 84, 6263–6270.
Wu, S., Duan, N., Wang, Z., Wang, H., 2011. Analyst 136, 2306–2314.
Wu, X., Hu, J., Zhu, B., Lu, L., Huang, X., Pang, D., 2011. J. Chromatogr. A 1218, 7341–7346.
Wu, Y., Zhan, S., Wang, F., He, L., Zhi, W., Zhou, P., 2012a. Chem. Commun. 48, 4459–4461.
Wu, Y., Zhan, S., Xing, H., He, L., Xua, L., Zhou, P., 2012b. Nanoscale 4, 6841–6849.
Wu, S., Duan, N., Shi, Z., Fang, C., Wang, Z., 2014. Anal. Chem. 86, 3100–3107.
Xiang, Y., Tong, A., Lu, Y., 2009. J. Am. Chem. Soc. 131, 15352–15357.
Yadav, R., Dwivedi, S., Kumar, S., Chaudhury, A., 2010. Food Environ. Virol. 2, 53–63.

Yang, C., Wang, Y., Marty, J.L., Yang, X., 2011. Biosens. Bioelectron. 26, 2724–2727.
Yang, W., Ratinac, K.R., Ringer, S.P., Thordarson, P., Gooding, J.J., Braet, F., 2010. Angew. Chem. Int. Ed. 49, 2114–2138.
Yin, P.T., Kim, T.H., Choi, J.W., Lee, K.B., 2013. Phys. Chem. Chem. Phys. 15, 12785–12799.
Yuan, J., Tao, Z., Yu, Y., Ma, X., Xia, Y., Wang, L., Wang, Z., 2014. Food Control 37, 188–192.
Yuan, T., Liu, Z.Y., Hu, L.Z., Xu, G.B., 2011. Chin. J. Anal. Chem. 39, 972–977.
Yun, W., Li, H., Chen, S., Tu, D., Xie, W., Huang, Y., 2014. Eur. Food Res. Technol. 238, 989–995.
Zhang, C., Johnson, L.W., 2009. Anal. Chem. 81, 3051–3055.
Zhang, L., Chang, H., Hirata, A., Wu, H., Xue, Q., Chen, M., 2013. ACS Nano 7, 4595–4600.
Zhou, L., Wang, J., Li, D., Li, Y., 2014. Food Chem. 162, 34–40.
Zhu, Y., Chandra, P., Song, K.M., Ban, C., Shim, Y.B., 2012. Biosens. Bioelectron. 36, 29–34.
Zhu, Z., Su, Y., Li, J., Li, D., Zhang, J., Song, S., Zhao, Y., Li, G., Fan, C., 2009. Anal. Chem. 81, 7660–7666.